ADVANCED TEM TECHNIQUES FOR ASSESSING THE POSSIBLE BIOGENIC ORIGIN OF METEORITIC MAGNETITE CRYSTALS. M. Weyland[1], P. A. Midgley[1], R. E. Dunin-Borkowski[1], R. B. Frankel[2] and P. R. Buseck[3], [1]Department of Materials Science and Metallurgy, University of Cambridge, Pembroke Street, Cambridge CB2 3QZ, UK, [2]Department of Physics, California Polytechnic State University, San Luis Obispo, California 93407, USA, [3]Departments of Geological Sciences and Chemistry/ Biochemistry, Arizona State University, Tempe, Arizona 85287-1404, USA.

Introduction: The most compelling evidence for the former presence of extraterrestrial life is provided by a small subset of magnetite (Fe_3O_4) crystals found in meteorite ALH84001 from Mars, which are reported to be similar to magnetite crystals synthesized by terrestrial magnetotactic bacteria [1, 2]. The conclusion that the meteoritic crystals are 'physically and chemically identical to … magnetites produced by magnetotactic bacteria strain MV-1' [3] is based on measurements of their three-dimensional morphologies using bright-field transmission electron microscopy (TEM). We have argued recently that more advanced techniques are required to establish whether such crystals, which are only ~50 nm in size, are identical to bacterial magnetite and thus biogenic in origin [4]. Here we illustrate these approaches by using them to characterize magnetite crystals from two strains of bacteria from Sweet Springs Nature Reserve, Morro Bay, CA. We are presently applying these methods to characterize magnetite crystals from MV-1 and ALH84001.

STEM HAADF electron tomography: The three-dimensional *morphology* of a magnetite crystal can be determined directly by using electron tomography [5]. A ±60° tilt series of images of the crystal is obtained using a technique such as high-angle annular dark field (HAADF) imaging in the scanning transmission electron microscope (STEM), which provides a signal that is proportional to sample thickness and depends on the local atomic number. Well-established algorithms are then used to reconstruct the morphology of the crystal from the tilt series. No assumptions are required about the symmetry of the crystal or about the faces that may be present. Images can be obtained without needing to orient the crystal to any particular zone axis, and a spatial resolution approaching 1 nm can be achieved in a $(100\ nm)^3$ volume [5]. An HAADF image taken from a tilt series of 57 images of two chains of magnetite crystals in a single bacterial cell is shown in Fig. 1a. A tomographic reconstruction of one of the crystals (arrowed in Fig. 1a) is shown from a range of directions in Fig. 1b. Six {110} faces are visible along the length of the crystal, with two large {111} faces at its ends and smaller {111} corner faces. Each crystal in Fig. 1a can be reconstructed in this way, providing statistical high-resolution information about 20-30 crystals from a single tilt series.

EFTEM electron tomography: Electron tomography can also be applied to energy-filtered (EF) TEM images to obtain three-dimensional information about the local *chemistry* both within a magnetite crystal and surrounding it (as well as about its morphology). An imaging spectrometer such as a Gatan Imaging Filter (GIF) is used to obtain chemical maps at sample tilt angles of up to ±60°. At each tilt angle, energy-loss images are acquired close to a core-loss edge of interest such as the Fe $L_{2,3}$ edge. Chemical maps are then calculated using techniques based on electron energy loss spectroscopy (EELS). Figures 2a and b show reconstructions (viewed from a single direction) of the three-dimensional distribution of O and Fe associated with a chain of magnetite crystals that are slightly smaller than those in bacterial strain MV-1. (The large white feature in Fig. 2a and in Fig. 3a below is a polyphosphate granule). The tilt series used to obtain Figs. 2a and b contained 156 images. The difference between these signals is shown in Fig. 2c. The enhancement in Fe at the edge of each crystal, which is mapped in three dimensions using this technique, provides unique information about the growth mechanisms of the crystals, and hence about their origin.

EFTEM image spectroscopy: If required, highly improved statistics about local chemistry are provided in the TEM by using "image spectroscopy" to record and analyze an extended series of energy-loss images [6]. This approach also allows multiple scattering contributions to the contrast to be deconvoluted from the data. Figures 3a and b show O and Fe elemental maps calculated from 80 energy-loss images of the chain shown in Fig. 2. The images were obtained at a single sample tilt, using a 10 eV wide energy-selecting slit, in 10 eV steps from 0 to 800 eV. Line traces (Fig. 3c) confirm the presence of O depletion at the edges of the crystals, as seen above (with poorer statistics) in Fig. 2.

References: [1] McKay D. S. et al. (1996) *Science, 273,* 924-930. [2] Thomas-Keprta K. L. et al. (2001) *Geochim. Cosmochim. Acta, 64,* 4049-4081. [3] Thomas-Keprta K. L. et al. (2001) *Proc. Natl. Acad. Sci. USA, 98,* 2164-2169. [4] Buseck P. R. et al. (2001) *Proc. Natl. Acad. Sci. USA, 98,* 13490-13495. [5] Midgley P. A. et al. (2001) *Chem. Commun., 10,* 907-908. [6] Thomas P. J. and Midgley P. A. (2001) *Utramicr., 88,* 179-186.

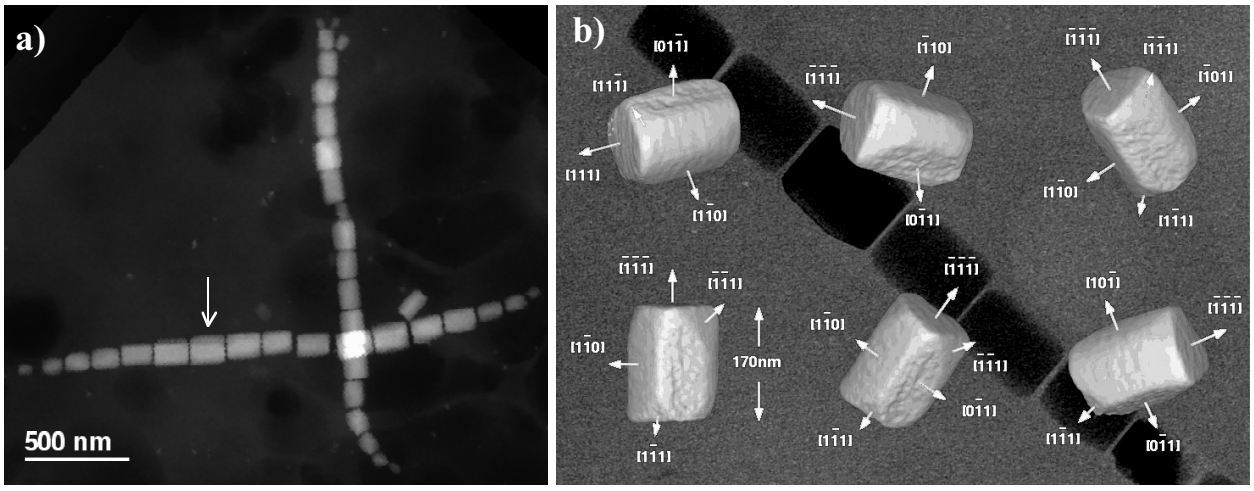

Figure 1. a) STEM HAADF image of magnetite chains in a coccus. b) Tomographic reconstruction of the crystal arrowed in a) obtained from a tilt series of 57 STEM HAADF images in a Philips CM300 field emission gun combined TEM/ STEM. The tableau shows the three-dimensional morphology of the crystal from several directions. A conventional bright-field image is shown in the background. (Fig. 1b is adapted from Fig. 3 in Ref. [4]).

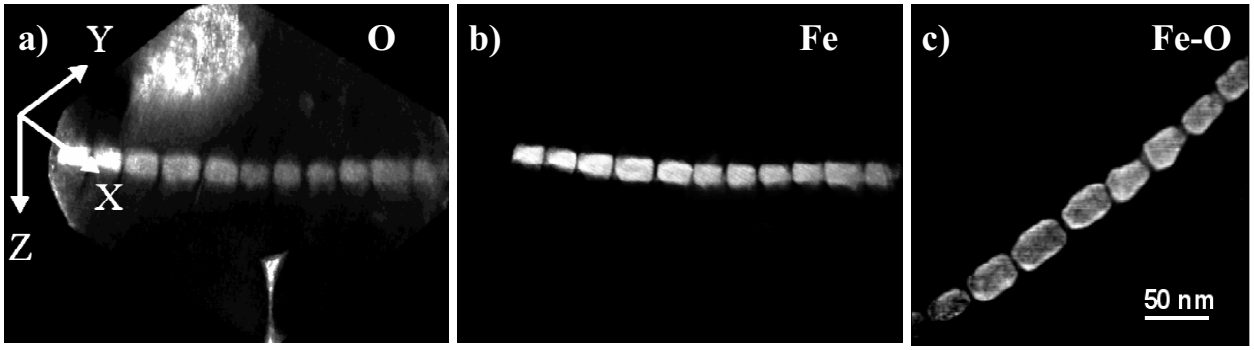

Figure 2. Three-dimensional a) O and b) Fe distributions for 40-nm magnetite crystals from a different strain of bacteria to that in Fig. 1. The images were obtained by applying tomographic reconstruction to a tilt series of 156 energy loss images. c) Difference between Fe and O signals showing an enhancement in Fe at the crystal edges.

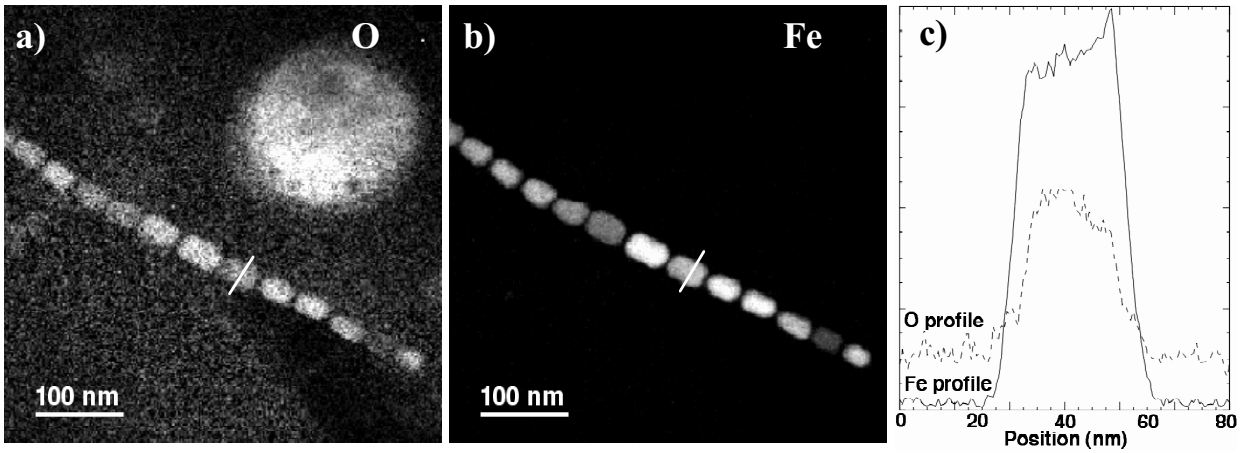

Figure 3. a) O and b) Fe elemental maps obtained from a spectrum image series of 80 energy loss images of the chain shown in Fig. 2 over an energy range of 0-800 eV. c) Line profiles across the crystal marked in a) and b), showing a drop in O concentration relative to that of Fe at the edges.